Int. J. Heat Mass Transfer. Vol. 11, pp. 1621–1636. Pergamon Press 1968. Printed in Great Britain

LAMINAR HEAT TRANSFER IN ELECTRICALLY CONDUCTING FLUIDS FLOWING IN PARALLEL PLATE CHANNELS*

L. H. BACK†

Jet Propulsion Laboratory, Pasadena, California, U.S.A.

(*Received* 6 *September* 1967 *and in revised form* 21 *February* 1968)

Abstract—Predicted wall heat fluxes, bulk fluid temperatures, and Nusselt numbers are presented in the thermal entrance region for a steady, constant-property, uniform laminar flow of an electrically conducting fluid in a constant cross-section, parallel-plate channel with isothermal, electrically nonconducting walls. Uniform magnetic and electric fields are applied perpendicular to each other and to the flow. The predictions, taking into account longitudinal heat conduction, depend upon location along the channel, the product of Reynolds and Prandtl numbers (*RePr*), and upon a Joule heating parameter *S*. The importance of Joule heating is displayed graphically. Thermal entrance lengths, proportional to *RePr*, decrease with Joule heating, and are of the order of the channel height for small *RePr*. Existing predictions of velocity entrance lengths are included for comparative purposes. The fully developed region is also discussed.

NOMENCLATURE

a, channel half-height;
B, magnetic field strength
c, specific heat;
e, internal energy;
E, electric field strength;
Ek, Eckert number, $\bar{u}^2/c(T_i - T_w)$;
F, body force;
h, local heat-transfer coefficient, $q_w/(T_b - T_w)$;
Ha, Hartmann number, $Ba\sqrt{(\sigma/\mu)}$;
j, electrical current;
k, thermal conductivity;
K, electric field factor, $E/\bar{u}B$;
l, channel length;
l_T, thermal entrance length;
l_v, velocity entrance length;
$\bar{l}$, nondimensional variable, $\dfrac{l}{2a}\dfrac{1}{RePr}$;
m_n, defined in equation (10);
n, integer;
Nu, local Nusselt number, $h2a/k$;
p, pressure;
Pr, Prandtl number, ν/α;
q, local heat flux;
$\bar{q}$, average heat flux for one wall of a channel of length l;
Re, Reynolds number based on channel height, $\bar{u}2a/\nu$;
S, Joule heating parameter; $Ha^2Ek(1 - K)^2Pr$;
T, temperature;
u, v, velocity components in the x and y directions, respectively;
$\bar{u}$, uniform flow velocity;
x, distance along channel from inlet;
$\bar{x}$, nondimensional variable, $\dfrac{x}{2a}\dfrac{1}{RePr}$;
y, distance across channel height;
z, distance perpendicular to x, y plane.

Greek symbols

α, thermal diffusivity, $k/\rho c$;
η, nondimensional distance, y/a;
θ, temperature difference ratio, $(T - T_w)/(T_i - T_w)$;
λ_n, eigenvalue, equation (10);
μ, viscosity;
ν, kinematic viscosity, μ/ρ;

* This paper presents the results of one phase of research carried out at the Jet Propulsion Laboratory, California Institute of Technology, under Contract No. NAS7-100, sponsored by the National Aeronautics and Space Administration.

† Senior Engineer, Jet Propulsion Laboratory, Pasadena, California.

ξ, nondimensional variable, $\frac{x}{a}\frac{1}{(ua/\alpha)}$;

ρ, density;
σ, electrical conductivity;
τ_{jk}, viscous stress tensor;
Φ, viscous dissipation.

Subscripts

b, bulk or average condition;
$\mathfrak{L}$, centreline;
i, channel inlet;
w, channel wall.

INTRODUCTION

INTEREST in laminar heat transfer in electrically conducting fluids flowing through channels spans a wide range of applications that can be divided into those involving electrical energy extraction or addition. In either case there is electrical dissipation by Joule heating, and the heat transfer is influenced by the applied field.

This paper presents a theoretical analysis of heat transfer in a steady, laminar, constant-property flow of an electrically conducting fluid through a parallel-plate channel with a uniform magnetic field applied perpendicular to the flow (Fig. 1). The analysis takes into account an applied electric field aligned with the electric field induced by the interaction of the applied magnetic field and the velocity of the fluid. The uniform electric field is applied across the flow to supply energy, or an external resistance is connected across the flow to extract energy. The parallel plates of the channel are taken to be electrically nonconducting and isothermal, and of a sufficiently large width-to-height ratio so that secondary flow effects arising as a result of the sidewalls are negligible. Flow along the sidewalls, taken to be perfectly conducting electrodes, is not treated; therefore, heat transfer to the electrodes is not studied in the analysis. A low magnetic Reynolds number is considered so that the induced magnetic field is negligible compared to the uniform applied magnetic field. Also, Hall currents, slip conditions, and non-equilibrium effects are not considered if the fluid is a gas.

Application of fields can influence the development of the temperature distribution along the channel in various ways. If the inlet temperature of the fluid is uniform, and the plates are isothermal, the convection of energy by the mean flow, viscous dissipation, and electrical dissipation by Joule heating are dependent on the velocity distribution. Electrical dissipation is also directly dependent on the strengths of the applied fields. Nondimensionalizing the thermal energy equation indicates the following parameters upon which the temperature distribution is dependent: velocity distribution; nondimensional distance along the channel involving the Reynolds–Prandtl number,

$$\frac{x}{2a}\frac{1}{RePr};$$

Hartmann number, $Ba\sqrt{(\sigma/\mu)}$; Prandtl number; Eckert number,

$$Ek = \frac{\bar{u}^2}{c(T_i - T_w)};$$

and ratio of the external electric field to the induced electric field,

$$K = \frac{E}{\bar{u}B},$$

($K < 1$ for energy extraction and $K > 1$ for energy addition).

With the velocity distribution specified, predictions of the temperature distribution in the

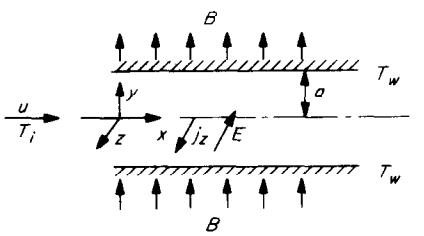

FIG. 1. Parallel-plate channel with transverse uniform magnetic field, uniform external electric field, and isothermal, electrically nonconducting walls.

thermal entrance region have been made by a number of investigators, but over a rather small range of parameters. Shohet *et al.* [1], using their calculated velocity distributions in the entrance region, predicted the temperature distributions with zero external resistance, $K = 0$ (short circuit case) for specific values of the Hartmann number of 4, Prandtl number of 0·1, and Eckert number of 1·0; no heat-transfer predictions were included. Erickson *et al.* [2], calculated the temperature distribution for fully developed Hartmann velocity profiles

$$\frac{u}{\bar{u}} = Ha\frac{[\cosh(Ha) - \cosh(Ha\, y/a)]}{[Ha\cosh(Ha) - \sinh(Ha)]} \quad (1)$$

for Hartmann numbers to 10, a Prandtl number of 1·0, Eckert number range from 0·1 to 1·0, and values of K from 0·5 to 1, with the value of $K = 1$ corresponding to the open circuit case. Both fluid bulk temperatures and average Nusselt numbers were presented graphically. Michiyoshi and Matsumoto [3], also using the fully developed Hartmann velocity profiles, obtained temperature distributions for Hartmann numbers up to 8, for certain values of a parameter defined in their paper, but only for $K = 1$. Local Nusselt numbers were shown graphically. Closed form solutions for the temperature distributions were obtained by Tan and Suh [4] who approximated the fully developed Hartmann velocity profiles by a step function for high Hartmann numbers. Unfortunately, the series solutions for the temperature distributions, wall heat fluxes, and Nusselt numbers were not evaluated numerically. A larger range of Hartmann numbers to 30, Prandtl numbers down to 0·01, and a parameter involving Joule heating were investigated by Dhanak [5] by the von Kármán–Pohlhausen method, but for no external applied electric field, $K = 0$. Local and average Nusselt numbers were presented graphically. As previously pointed out in the literature, an earlier analysis by Nigam and Singh [6] contains an error in the Joule heating term.

Although these analyses are useful in a particular application for the range of parameters to which they apply, there is a need for solutions that indicate the effect of applied fields on heat transfer over a greater range of the numerous parameters. Solutions should be presented graphically to display the results and include, besides Nusselt numbers, predicted wall heat fluxes and fluid bulk temperatures, useful relations for application purposes. The purpose of this paper is to attempt to provide such solutions. The basic assumption in the analysis is with regard to the velocity distribution. If the velocity distribution is uniform at the channel inlet, and if an increase in the Hartmann number causes the fully developed velocity profile to become uniform across the channel (see various sources, e.g. Sutton and Sherman [7], p. 346), it appears that taking the velocity profile as uniform across the channel in the thermal entrance region is a reasonable approximation that becomes more exact as the Hartmann number increases. Such an approximation is called uniform or slug flow, and forms the basis of this analysis. In addition, longitudinal heat conduction not considered in the previously mentioned analyses, except in [6], is included. Schneider [8], in predicting laminar heat transfer in the thermal entrance region of uniform velocity flows through channels without fields, has shown that longitudinal heat conduction is important for values of $RePr$ below approximately 100. Consequently, longitudinal heat conduction is expected to be important for liquid metals that have small Prandtl numbers over a substantial Reynolds number range for laminar flow. It can also be important in gas flows. For the special case of a completely ionized gas, predicted Prandtl numbers are small, on the order of 0·01 (de Voto [9]), a value of the same order of magnitude as liquid metals.

In the subsequent sections, solutions of the thermal energy equation are obtained and the nondimensional wall heat fluxes, fluid bulk-to-wall temperature ratios, and Nusselt numbers are presented graphically. These quantities

depend on (1) the nondimensional distance along the channel, (2) Reynolds–Prandtl number, and (3) Joule heating parameter. Thermal entrance lengths are presented and compared with velocity entrance lengths. In the last section, these solutions are discussed in connection with fully developed thermal solutions in which the Hartmann velocity profiles are utilized, and some limitations are indicated for values of the external electric field near the induced electric field

ANALYSIS

For steady, two-dimensional laminar flow of a constant-property, electrically conducting fluid through a parallel plate channel with externally applied uniform fields (Fig. 1), the thermal energy equation

$$\rho \frac{De}{Dt} + p \frac{\partial u_j}{\partial x_j} = - \frac{\partial}{\partial x_j}(q_j) + \Phi + \frac{j^2}{\sigma} \quad (2)$$

becomes

$$\rho \bar{u} c \frac{\partial T}{\partial x} = k \left[\frac{\partial^2 T}{\partial x^2} + \frac{\partial^2 T}{\partial y^2} \right] + \sigma \bar{u}^2 B^2 [1 - K]^2. \quad (3)$$

In this form, the following considerations are implied:

(1) Internal energy, $e = cT$.

(2) Compression work,

$$p \frac{\partial u_j}{\partial x_j} = 0,$$

since from the continuity equation for a constant property flow,

$$\frac{\partial u_j}{\partial x_j} = 0.$$

(3) Transverse velocity $v = 0$, which implies $u(y)$ from the continuity equation. The uniform flow approximation is $u = \bar{u}$, and for a channel with a constant cross-section, $\bar{u}$ = constant along the channel.

(4) Fourier heat conduction,

$$q_j = - k \frac{\partial T}{\partial x_j}.$$

(5) Viscous dissipation

$$\Phi = \tau_{jk} \frac{\partial u_j}{\partial x_k} = 0,$$

as a result of no velocity gradients.

(6) Ohm's law, $j = j_z = \sigma[\bar{u}B - E]$.

The longitudinal heat-conduction term is

$$k \frac{\partial^2 T}{\partial x^2}.$$

Consequences of the uniform flow approximation are that heat is generated uniformly across the channel by electrical dissipation, viscous dissipation vanishes, and the momentum equation,

$$\rho \frac{Du_j}{Dt} = - \frac{\partial p}{\partial x_j} + \frac{\partial}{\partial x_k}(\tau_{jk}) + F_j \quad (4)$$

reduces to a balance between the pressure gradient and the Lorentz force in the flow direction

$$- \frac{\partial p}{\partial x} = j_z B$$

with momentum changes and viscous stresses vanishing. By introducing the nondimensional spatial variables, η and ξ, with a, the channel half-height, and α, the thermal diffusivity

$$\eta = \frac{y}{a}$$

$$\xi = \frac{x}{a} \frac{1}{(\bar{u}a/\alpha)}$$

and the temperature difference ratio,

$$\theta = \frac{T - T_w}{T_i - T_w}$$

the thermal energy equation becomes

$$\frac{\partial \theta}{\partial \xi} = \frac{1}{(\bar{u}a/\alpha)^2} \frac{\partial^2 \theta}{\partial \xi^2} + \frac{\partial^2 \theta}{\partial \eta^2} + S. \quad (5)$$

The Joule heating parameter is S, where $S = Ha^2 Ek(1 - K)^2 Pr$. For the thermal energy

equation in this form, $\theta = 1$ at the channel inlet ($\xi = 0$) where the temperature is at a uniform value T_i, and $\theta = 0$ at $\eta = 1$, along the isothermal plates at temperature T_w. If the inlet temperature is taken as uniform, any nonuniformity in temperature upstream of the channel inlet that could result from permitting longitudinal heat conduction in the inlet region is not considered. From symmetry considerations, $\partial\theta/\partial\eta = 0$, along the centerline ($\eta = 0$).

The solution of equation (5) is constructed in two parts. If the temperature difference ratio where longitudinal gradients vanish is denoted by θ_2, i.e. in the fully developed region, equations (5) becomes

$$\frac{d^2\theta_2}{d\eta^2} + S = 0.$$

Integration of this equation and satisfaction of the conditions $\theta_2 = 0$ at $\eta = 1$ and $d\theta_2/d\eta = 0$ at $\eta = 0$ gives

$$\theta_2 = \frac{S}{2}(1 - \eta^2). \tag{6}$$

Introduction of a temperature difference ratio, θ_1, that is to be added to the fully developed solution to obtain the temperature distribution in the thermal entrance region, gives

$$\theta = \theta_1 + \theta_2 = \theta_1 + \frac{S}{2}(1 - \eta^2).$$

Substituting this relation into equation (5) results in the following differential equation for θ_1 and the corresponding boundary conditions

$$\frac{\partial\theta_1}{\partial\xi} = \frac{1}{(\bar{u}a/\alpha)^2}\frac{\partial^2\theta_1}{\partial\xi^2} + \frac{\partial^2\theta_1}{\partial\eta^2} \tag{7}$$

at $\xi = 0$

$$\theta_1 = 1 - \frac{S}{2}(1 - \eta^2)$$

at $\eta = 1$

$$\theta_1 = 0 \tag{8}$$

at $\eta = 0$

$$\frac{\partial\theta_1}{\partial\eta} = 0.$$

The solution of equation (7), satisfying the boundary conditions given in equation (8), is obtained by separation of variables. The complete solution is obtained by adding this solution to the solution for fully developed flow.

$$\theta = \frac{S}{2}(1 - \eta^2) + 2\sum_{n=0}^{\infty}\frac{(-1)^n}{\lambda_n}\left(1 - \frac{S}{\lambda_n^2}\right)\exp(-m_n\bar{x})\cos(\lambda_n\eta) \tag{9}$$

where

$$m_n = (RePr)\left\{\left[\left(\frac{RePr}{2}\right)^2 + 4\lambda_n^2\right]^{\frac{1}{2}} - \frac{(RePr)}{2}\right\} \tag{10}$$

and

$$\lambda_n = (2n + 1)\frac{\pi}{2}.$$

The group $\bar{u}a/\alpha$ (often referred to as the Péclet number) and nondimensional length variable have been written as

$$\frac{\bar{u}a}{\alpha} = \tfrac{1}{2}RePr$$

and

$$\xi = 4\bar{x}$$

where

$$\bar{x} = \frac{x}{2a}\frac{1}{RePr}.$$

By so doing, the distance along the channel and Reynolds number are referenced to the channel height, $2a$, rather than the half-height, a.

Once the temperature distribution is known, the thermal quantities of interest are as follows: The local wall heat flux, $-k(\partial T/\partial y)_w$, in nondimensional form is

$$\frac{q_w}{(T_i - T_w)}\frac{2a}{k} = -2\left(\frac{\partial\theta}{\partial\eta}\right)_w = 2S + 4\sum_{n=0}^{\infty}\left(1 - \frac{S}{\lambda_n^2}\right)\exp(-m_n\bar{x}). \quad (11)$$

The fluid bulk or average temperature difference ratio for a uniform flow is obtained from equation (9)

$$\theta_b = \int_0^1 \theta\,d\eta = \frac{S}{3} + 2\sum_{n=0}^{\infty}\frac{1}{\lambda_n^2}\left(1 - \frac{S}{\lambda_n^2}\right)\exp(-m_n\bar{x}). \quad (12)$$

Defining a local heat-transfer coefficient by

$$h = \frac{q_w}{(T_b - T_w)},$$

the local Nusselt number can be written in terms of these quantities as

$$Nu = \frac{h2a}{k} = -\frac{\left(\frac{\partial\theta}{\partial\eta}\right)_w}{\int_0^1 \theta\,d\eta} = \frac{2S + 4\sum_{n=0}^{\infty}\left(1 - \frac{S}{\lambda_n^2}\right)\exp(-m_n\bar{x})}{\frac{S}{3} + 2\sum_{n=0}^{\infty}\frac{1}{\lambda_n^2}\left(1 - \frac{S}{\lambda_n^2}\right)\exp(-m_n\bar{x})}. \quad (13)$$

The average heat flux for one wall of a channel of length l, is

$$\bar{q}_w = \frac{1}{l}\int_0^l q_w\,dx,$$

is obtained by integrating equation (11) as follows:

$$\frac{\bar{q}_w}{(T_i - T_w)}\frac{2a}{k} = 2S + 4\sum_{n=0}^{\infty}\left(1 - \frac{S}{\lambda_n^2}\right)\frac{1}{m_n\bar{l}}[1 - \exp(-m_n\bar{l})] \quad (14)$$

where

$$\bar{l} = \frac{l}{2a}\frac{1}{RePr}.$$

The series in equations (11–14) were evaluated on an IBM 7094 computer over a substantial range of the parameters $\bar{x}$, $RePr$ and S. Values of $\bar{x}$ range from 10^{-4} to 10; values of $RePr$ from one to sufficiently high values, so that axial conduction was essentially negligible in the region of interest; and values of S from 0·01 to 100 (Figs. 2–7). Whereas for large values of $\bar{x}$ the first term in the series was sufficient, as many as 12000 terms were required for four-place accuracy at a small value of $\bar{x} = 10^{-4}$. The computer time for all calculations, however, was approximately 10 min.

THERMAL ENTRANCE REGION RESULTS

The predictions are graphically presented first for the case of negligible longitudinal heat conduction. The importance of longitudinal heat conduction is contained in m_n equation (10). For large values of $RePr$, m_n is related to λ_n by $m_n = 4\lambda_n^2$, a relation that is obtained from the solution of equation (5) without the longitudinal heat-conduction term, and the solution for the temperature distribution across the flow equation (9) depends only on the nondimensional variable $\bar{x}$, and Joule heating parameter S. Figure 2 indicates the variation of the nondimensional local wall heat flux with $\bar{x}$ for various values of S for negligible longitudinal heat conduction. At small values of $\bar{x}$, the predictions approach the solution for uniform flow over an isothermal flat plate with no applied field ($S = 0$) (Eckert and Drake [10]). This prediction in this representation is

$$\frac{q_w}{(T_i - T_w)}\frac{2a}{k} = \frac{1}{(\pi)^{\frac{1}{2}}}\left(\frac{x}{2a}\frac{1}{RePr}\right)^{-\frac{1}{2}}. \quad (15)$$

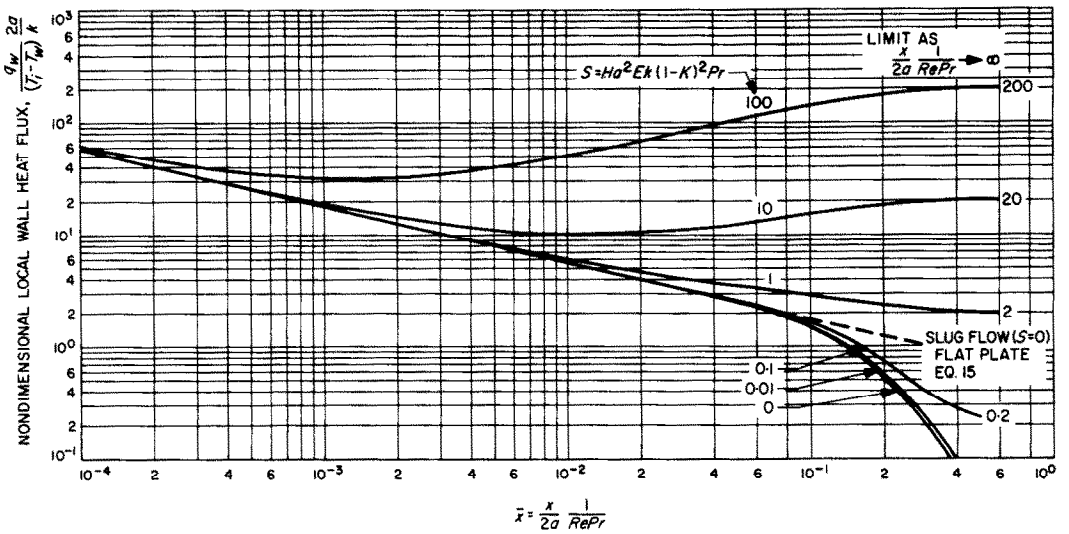

FIG. 2. Nondimensional local wall heat flux distributions in the thermal entrance for negligible longitudinal heat conduction

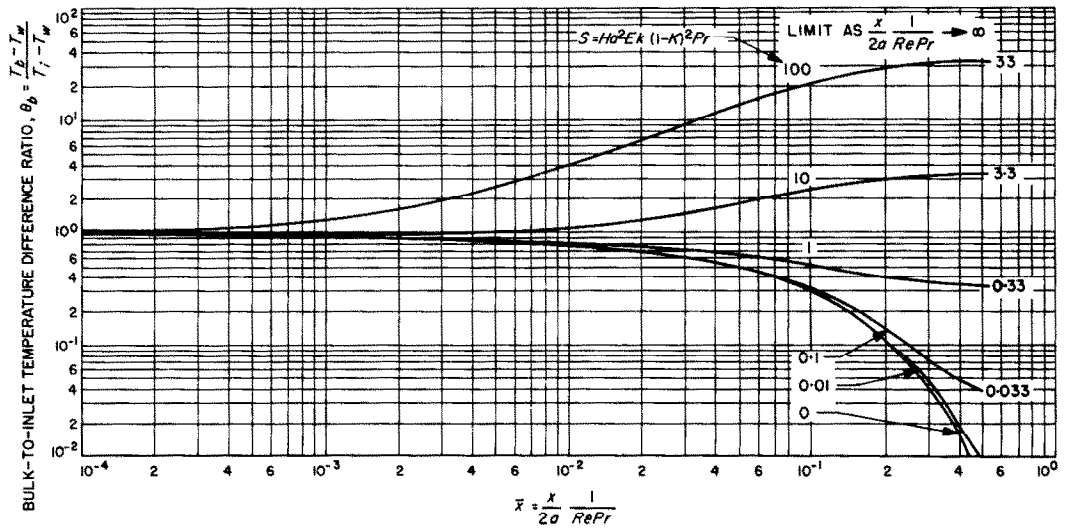

FIG. 3. Local fluid bulk to inlet temperature difference ratios in the thermal entrance region for negligible longitudinal head conduction

At larger values of $\bar{x}$, the predictions for small values of S lie below the flat plate prediction because the driving potential is less than the difference $(T_i - T_w)$ just downstream of the channel inlet. As S increases, the strong dependence of the wall heat flux on Joule heating is evident. At larger values of S, the wall heat flux decreases and reaches a minimum; then it increases along the channel, rather than continuing to decrease. This behavior can be visualized by constructing a solution of the linear energy equation in a different way than treated in the previous section. This solution consists of two parts. The first part of this solution satisfies the initial condition $(T_i - T_w)$ and wall condition $T_w = 0$ with no Joule heating. For the second part, the uniform inlet temperature T_i is equal to the wall temperature T_w,

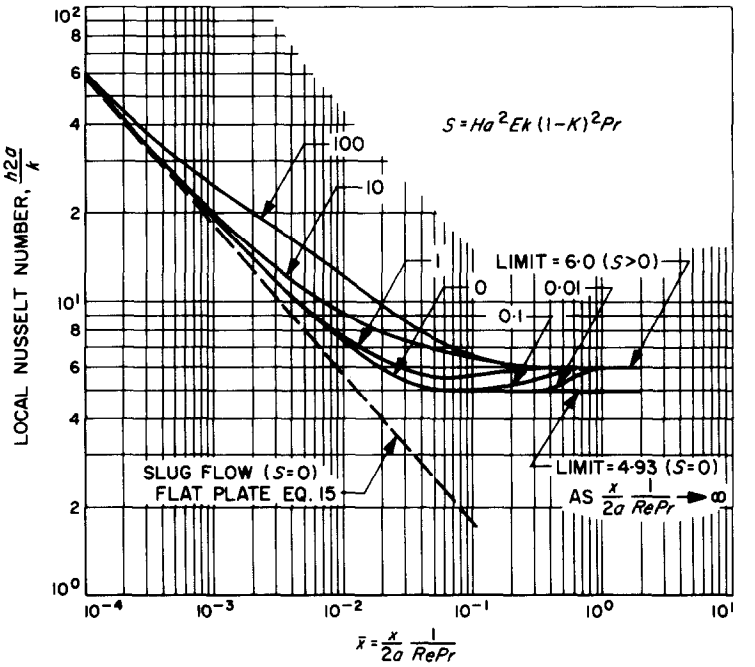

FIG. 4. Local Nusselt numbers in the thermal entrance region for negligible longitudinal heat conduction.

and Joule heating is included. The wall heat flux from the first part will decrease along the channel; however, for the second part, it will increase along the channel as a result of Joule heating. Consequently, the total wall heat flux, the sum of the two solutions, exhibits the trend shown in Fig. 2. This occurs whether longitudinal heat conduction is included or not. In Fig. 2, sufficiently far downstream of the channel inlet, heat conducted to the wall becomes equal to the electrical dissipation with the asymptotic value from either equations (6) or (11) being

$$\frac{q_w}{(T_i - T_w)}\frac{2a}{k} = 2S$$

or

$$\frac{q_w}{\bar{u}^2\mu/2a} = 2Ha^2(1 - K)^2. \tag{16}$$

A discussion of this fully developed value is presented subsequently.

The fluid bulk-temperature difference ratio, shown in Fig. 3 for negligible longitudinal heat conduction, displays trends similar to the wall heat flux. With no Joule heating, the ratio decreases along the channel as the fluid bulk temperature tends toward the wall temperature ($\theta_b \to 0$) as a result of convective energy loss from the flow by heat conduction to the wall. With Joule heating, this is no longer the case, and the fluid bulk temperature ratio from either equations (6) or (12) asymptotically approaches the value

$$\frac{T_b - T_w}{T_i - T_w} = \frac{1}{3}S. \tag{17}$$

The variation of the local Nusselt number with $\bar{x}$ for various values of S is shown in Fig. 4 for negligible longitudinal heat conduction. For small values of $\bar{x}$, where the fluid bulk temperature ratios differ slightly from unity, the Nusselt number essentially reflects the variation in wall heat flux and agrees with those values predicted from the flat plate relation equation (15). For small values of S, the heat flux prediction from equation (15) was in agreement with the wall

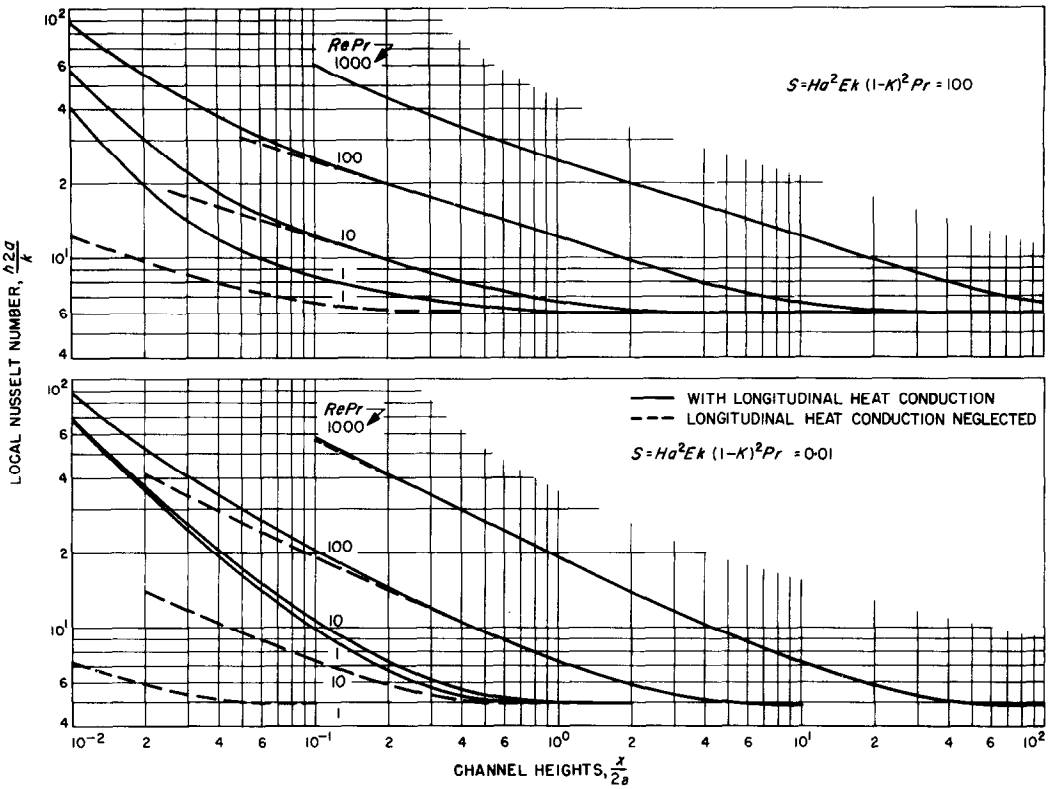

FIG. 5. Local Nusselt numbers along the channel in the thermal entrance region.

heat flux predictions shown in Fig. 2 for values of $\bar{x}$ up to approximately 10^{-1}, whereas the prediction from equation (15) is considerably below the channel flow Nusselt number predictions at this same value of $\bar{x}$. In this connection, it should be noted that for flat plate flow, the driving potential is between the free-stream and wall temperature which is $T_i - T_w$ just downstream of the channel inlet. The large discrepancy in the Nusselt number representation occurs because, at $\bar{x} = 10^{-1}$, the fluid bulk to inlet temperature ratio at small values of S has decreased to approximately 0·3 (Fig. 3). This is significant because the wall heat flux prediction from the flat plate relation remains a good approximation of the actual channel flow value for a larger value of $\bar{x}$ than is implied from observing the variation of the local Nusselt number. This is true even though the temperature along the centerline has decreased below the inlet temperature; in particular at $\bar{x} = 10^{-1}$, the ratio $(T_{\mathbb{Q}} - T_w)/(T_i - T_w)$ is approximately 0·5 for small values of S.

As $\bar{x}$ increases, the effect of Joule heating on the local Nusselt number becomes more pronounced (Fig. 4). The predictions merge toward the asymptotic value bf six, terminating the thermal entrance region. A local minimum in the Nusselt number at a value of $\bar{x} \cong 0{\cdot}05$ is evident for small values of S, where there is a tendency for the Nusselt number to locally approach the asymptotic value of 4·93 without Joule heating ($S = 0$). To place these asymptotic values in perspective, the asymptotic values of the Nusselt number for flow between isothermal plates without Joule heating and a fully developed parabolic velocity profile is 3·80 (Norris and Streid [11]). The value of 3·80 is approximately 25 per cent below the value for uniform flow without Joule heating.

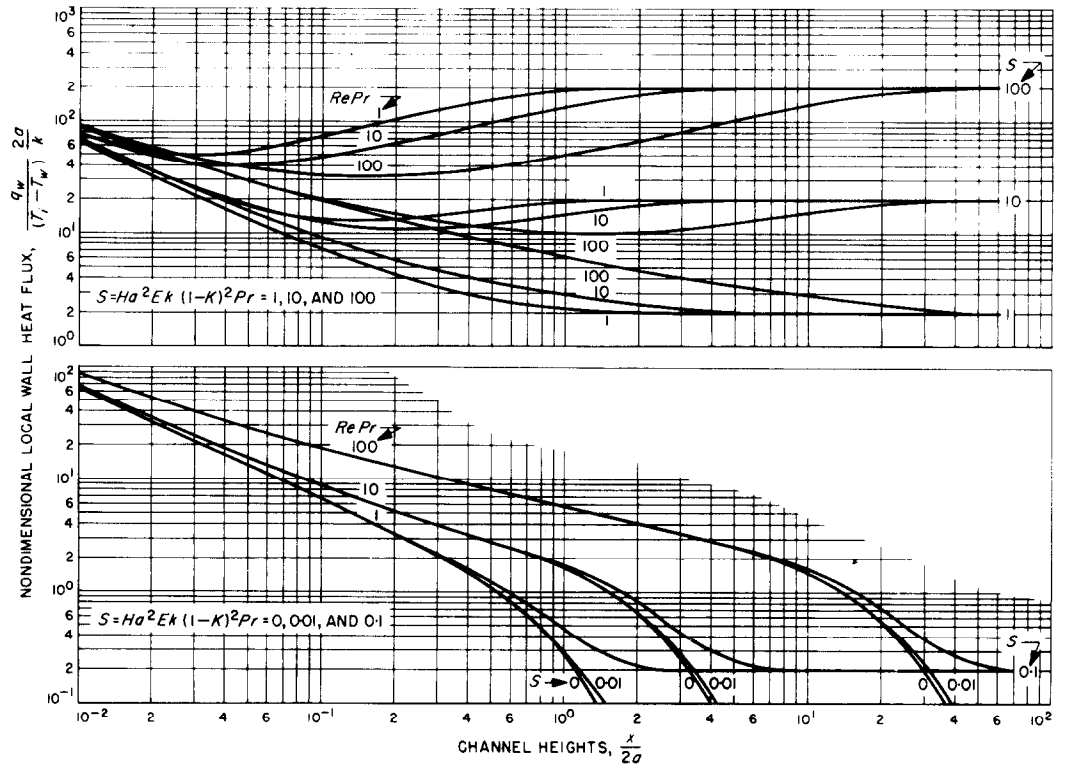

FIG. 6. Nondimensional local wall heat flux distributions along the channel in the thermal entrance region, including longitudinal heat conduction.

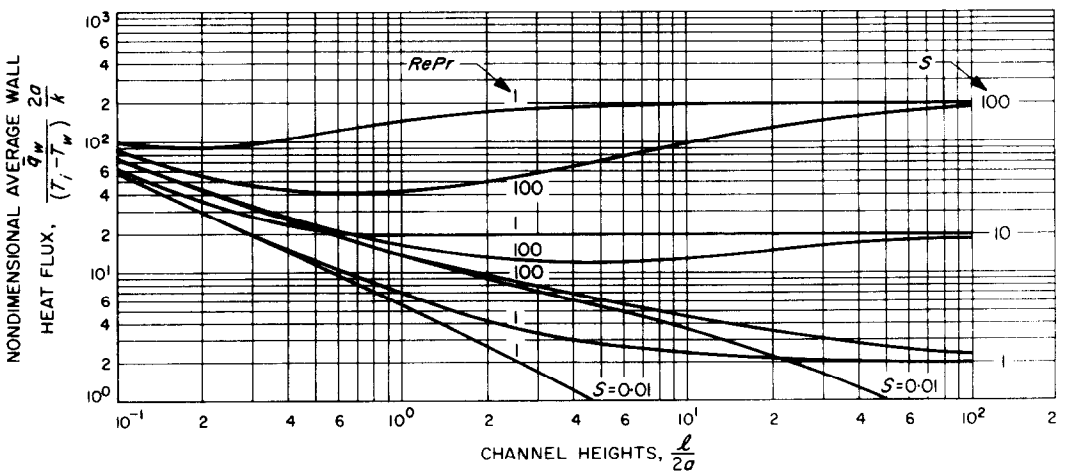

FIG. 7. Nondimensional average wall heat flux distributions, including longitudinal heat conduction.

Figures 2 and 3 indicate the magnitude of the variation of the wall heat fluxes and bulk-temperature difference ratios with S. These large variations are not evident if only the Nusselt number variation is presented, such as in Fig. 4.

Where longitudinal heat conduction is important, the thermal quantities of interest depend upon $RePr$, in addition to $\bar{x}$ and S. Alternately, since $RePr$ appears as a product in $\bar{x}$, the prediction can be taken to depend upon the channel height ratio $x/2a$, $RePr$, and S. In this representation, the results can be viewed along the channel in terms of channel heights, with $RePr$ and S as parameters.

The importance of longitudinal heat conduction is shown in Fig. 5 where the local Nusselt number variation along the channel is presented for a small and large value of S over a range of $RePr$ from 1 to 1000. At the lower values of $RePr$, where the thermal entrance region is on the order of the channel height, allowing for longitudinal heat conduction leads to significantly higher predicted Nusselt numbers than when it is neglected. For negligible Joule heating, this occurs because more energy is transferred by longitudinal heat conduction into an element Δx along the channel than out of the element when the wall is cooled. Consequently, the heat transfer to the wall is larger, as also is the Nusselt number. The heat transfer from a heated wall also increases when longitudinal heat conduction is included. In this case, heat is conducted upstream, with more heat conducted out than in, to balance the higher heat transfer from the wall. The inclusion of longitudinal heat conduction also decreases the longitudinal temperature gradient and, therefore, the convection of energy, $\rho\bar{u}c\,\partial T/\partial x$, by the flow. When Joule heating is large enough so that the fluid bulk temperature increases along the channel, heat is conducted upstream; however, for the cooled wall case, more heat is conducted in than out of the element and, again, heat transfer to the wall is larger. In Fig. 5, at the lower values of $RePr$, the thermal entrance lengths, in terms of channel heights, increase appreciably above the shorter lengths indicated by neglecting longitudinal heat conduction. For channel heights larger than 0·1, longitudinal heat conduction is important for values of $RePr$ less than approximately 100 at a small value of $S = 0{\cdot}01$. As S increases, the effect is less, with longitudinal heat conduction becoming important only for values of $RePr$ less than approximately ten at $S = 100$. For clarity, values of the Nusselt number beyond the location where it is a minimum (Fig. 4) are not shown in Fig. 5 for $S = 0{\cdot}01$.

The variation of the nondimensional wall heat flux, including longitudinal heat conduction, is shown in Fig. 6 along the channel over a range of S from 0 to 100 and at values of $RePr$ of 1, 10 and 100. The effect of $RePr$ on the wall heat flux is evident at a given value of S. For small values of S, the wall heat flux, at a location along the channel, increases with $RePr$ as expected. However, at larger values of Joule heating, the reverse can be true, with the wall heat flux decreasing with $RePr$. This situation arises when Joule heating becomes important relative to convection of energy, $\rho\bar{u}c\,\partial T/\partial x$. For a particular fluid, $RePr$ is proportional to the mass flux, $\rho\bar{u}$. Therefore, as $RePr$ decreases for a given value of S, less energy is convected downstream, and, consequently, more of the energy dissipated by Joule heating is conducted to the wall. To maintain the same value of S, the fields would have to be adjusted since $S \propto [\bar{u}^2B^2(1 - K)^2]$.

The nondimensional average wall heat flux for the channel is of importance for application purposes. These values are shown in Fig. 7, including longitudinal heat conduction, over a range of S from 0 to 100 and at values of $RePr$ of 1 and 100. The trends are similar to to those exhibited by the local heat flux.

THERMAL AND VELOCITY ENTRANCE LENGTHS

The extent of the thermal entrance region is shown in Fig. 8 in terms of the number of

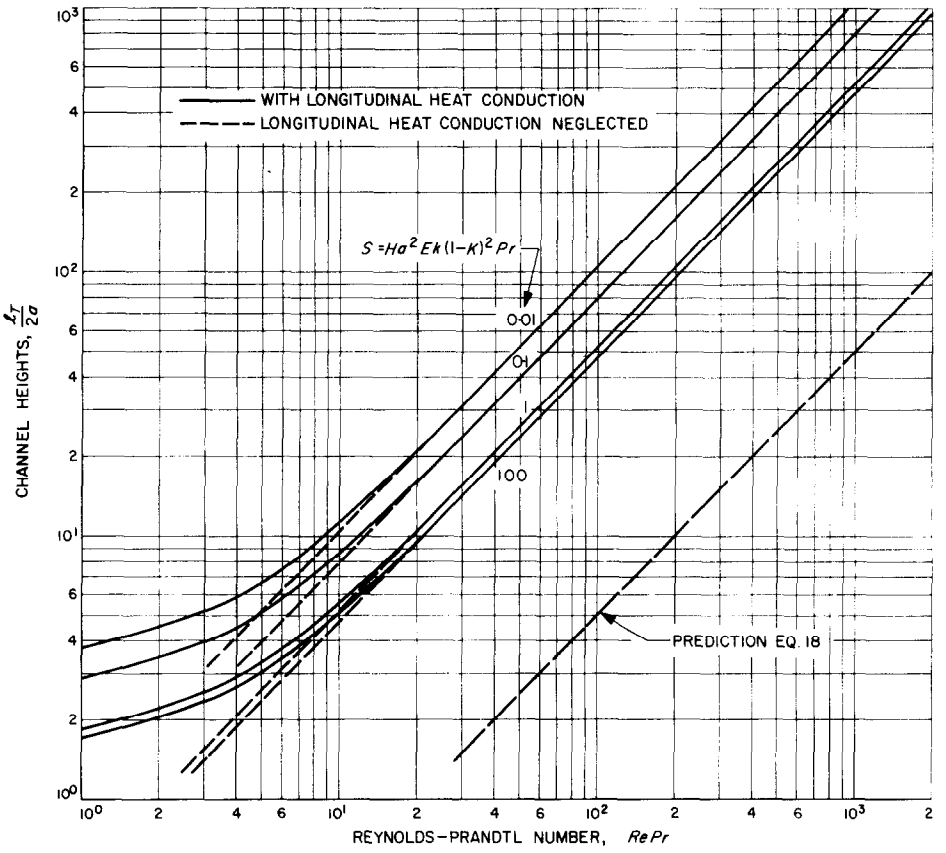

FIG. 8. Thermal entrance lengths. The curves correspond to locations where the fluid bulk-to-inlet temperature difference ratio is within 1 per cent of the fully developed thermal value.

channel heights to the location where the temperature difference ratio $(T_b - T_w)/(T_i - T_w)$ is within 1 per cent of the asymptotic value (a different percentage could be used as well). For small values of $RePr$, the entrance lengths are of the order of the channel height. Neglecting longitudinal heat conduction would lead to values that are too low in this region. As $RePr$ increases, the entrance lengths increase linearly with $RePr$. The entrance lengths decrease as Joule heating increases, although not significantly, over the large range of S shown. The following relation, which appears in the literature, e.g. Giedt [12] for no external fields, is also shown in Fig. 8.

$$\frac{l_T}{2a} \cong 0{\cdot}05\,(RePr). \tag{18}$$

This relation lies considerably below the other predictions primarily because of the basis on which the thermal entrance length is chosen. It corresponds to the location where the local Nusselt number becomes invariable with distance along the channel which, as in Fig. 4 (curve for $S = 0$), would yield the result given by equation (18). However, at

$$\frac{x}{2a}\frac{1}{RePr} = 0{\cdot}05,$$

both the wall heat flux and bulk temperature difference ratio are still changing appreciably with distance for all values of S (Figs. 2 and 3). The bulk temperature difference ratio is not within 1 per cent of its asymptotic zero value

until $(x/2a)(1/RePr) \cong 0{\cdot}5$ (Fig. 3, $S = 0$), a value more nearly in agreement with the predictions shown in Fig. 8. With Joule heating, entrance lengths calculated on a Nusselt number basis would also increase, and be similar to those lengths calculated on the bulk temperature basis.

Brief mention should be made of velocity entrance lengths that have been predicted for a uniform velocity profile at the channel inlet, and their relation to thermal entrance lengths. As the Hartmann number increases, predicted velocity entrance lengths [1, 13–16] for Hartmann numbers up to ten, decrease below the following relation for no external fields

$$\frac{l_v}{2a} \cong 0{\cdot}05\,(Re) \tag{19}$$

solutions that are implied by the uniform flow assumption, the fully developed thermal region is considered. In this region, longitudinal gradients vanish and the thermal energy, equation (2), becomes

$$0 = k\frac{d^2T}{dy^2} + \mu\left(\frac{du}{dy}\right)^2 + \sigma\bar{u}^2B^2\left(\frac{u}{\bar{u}} - K\right)^2. \tag{21}$$

For the fully developed Hartmann velocity profiles, Sutton and Sherman [7], p. 348, have given the solution to equation (21) for the temperature distribution from which the wall heat flux can be written in the following form (also see an earlier solution by Romig [19] for the wall heat flux where Romig's K is $(-K)$ herein):

$$\frac{q_w}{\bar{u}^2\mu/2a} = 2Ha^2\left\{(K-1)^2 + \frac{1}{2}\frac{Ha\sinh(2Ha) - \cosh(2Ha) + 1}{[Ha\cosh(Ha) - \sinh(Ha)]^2}\right\}. \tag{22}$$

and are in agreement with Shercliff's prediction [17] for large Hartmann numbers

$$\frac{l_v}{2a} = \frac{1}{4}\frac{Re}{Ha^2}. \tag{20}$$

A few solutions of the full Navier–Stokes equations by Brandt and Gillis [18] do, however, indicate longer entrance lengths than the small fractional values that might be predicted from equation (20) for large Hartmann numbers when the Reynolds number is not large.

The relative relation between the thermal and velocity entrance lengths l_T/l_v becomes of order unity at large Hartmann numbers for a small Prandtl number fluid. This is unlike the situation with no external fields where l_T/l_v is of the order of the Prandtl number. For a fluid with Prandtl number of order unity, l_T exceeds l_v, with the ratio l_T/l_v increasing with Hartmann number.

FULLY DEVELOPED REGION

To gain some insight into the limitations of the

Predictions from equation (22) are shown by the solid curves in Fig. 9 as a function of Hartmann number for various values of the electric field factor K. The magnitude of the factor K depends on the relative amount of electrical energy extraction or addition. For energy extraction, $K < 1$, the heat-transfer group decreases with increasing K since the current, and therefore the Joule heating, decreases. For energy addition, $K > 1$, the heat-transfer group increases with increasing K, since Joule heating increases. An indication of the fully developed predictions for a uniform velocity profile from equation (16) is shown in Fig. 9 by the dashed curves. For values of K not near unity, the applicability of these predictions in terms of Hartmann number is as indicated. For example, for $K = 0$ or 2, the predictions are within 10 per cent of the value from equation (22) for Hartmann numbers of ten and higher. At higher values of K, the agreement is better, being within 10 per cent at Hartmann numbers of three and higher for $K = 4$. However, for values of K near unity,

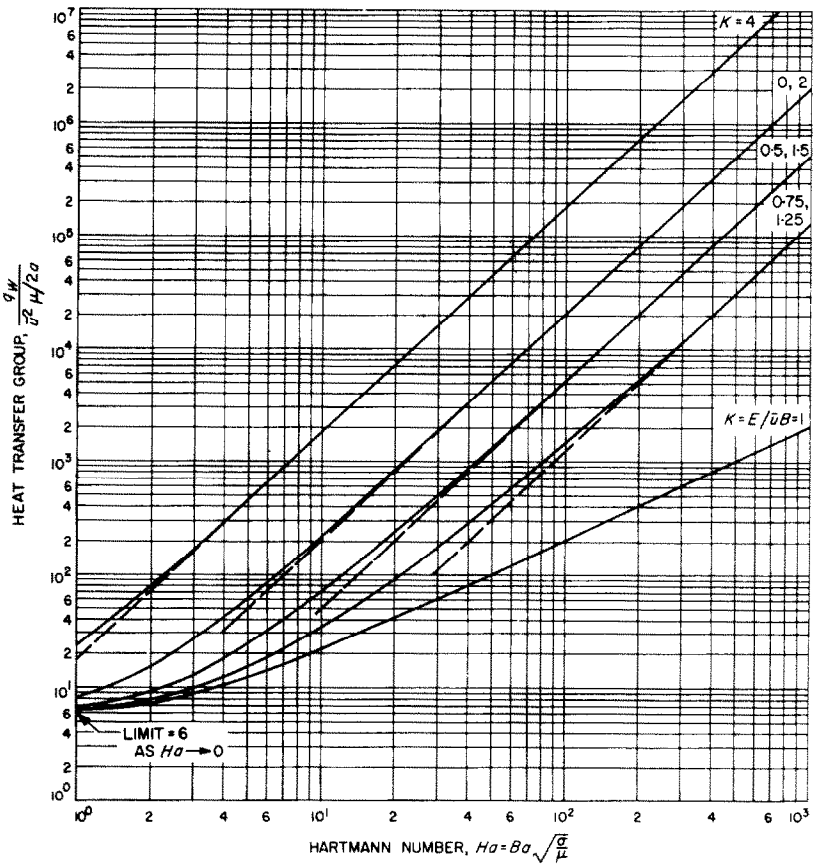

FIG. 9. Heat-transfer group for fully developed flow. The solid curves are predictions using the Hartmann velocity profiles, equation (22), and the dashed curves are for uniform flow, equation (16).

limitations on the fully developed thermal predictions are apparent in that part of the channel where the velocity distribution approaches the fully developed Hartmann profile. For this condition, the predicted electrical dissipation is less and is sensitive to the assumption of uniform flow, such as existed at the channel inlet. Viscous dissipation, absent in a uniform flow, also becomes important when it is comparable to electrical dissipation, such as is the case for values of K near unity and small Hartmann numbers. Consequently, for the values of K near unity, a better description of the velocity distribution is required for the solution of the thermal energy equation. In principle, the predicted velocity distributions in the flow development region [13–16] could be used. If the flow is fully developed, the predictions by Erickson *et al.* [2], for values of K from 0·5 to 1 (a range of interest for generators), Prandtl number of 1·0 and Hartmann numbers to ten are available. The predictions of Michiyoshi and Matsumoto [3] for $K = 1$ should be regarded with caution since viscous dissipation was neglected in the relatively low Hartmann number range of their investigation.

CONCLUSION

Predicted wall heat fluxes, fluid bulk-to-wall temperature ratios, and Nusselt numbers have been presented in the thermal entrance region of a parallel-plate channel with isothermal,

electrically nonconducting walls. The fluid is electrically conducting and has constant properties. Laminar flow was considered with a uniform velocity distribution and with magnetic and electric fields applied perpendicular to each other and to the fluid velocity. These predictions, which take into account longitudinal heat conduction, important when the thermal entrance region is of the order of the channel height, are dependent upon the location along the channel, the product of the Reynolds and Prandtl numbers, and upon the Joule heating parameter. Graphical presentation of the results over a large range of these parameters illustrates the role of Joule heating in increasing the heat transfer at various values of $RePr$.

Thermal entrance lengths l_T were proportional to $RePr$, similar to the case of no applied fields. Additionally, these lengths decreased with an increase in Joule heating. For small values of $RePr$, values of l_T are of the order of the channel height. Relative to predicted velocity entrance lengths l_v at large Hartmann numbers, the ratio l_T/l_v becomes of order unity for small Prandtl numbers, whereas with no external fields, l_T/l_v is of the order of the Prandtl number.

Consideration of more exact solutions for the temperature distribution in the fully developed region that incorporate the Hartmann velocity profiles, indicates limitations on the uniform flow predictions for values of the external electric field near the induced electric field. For this case, in that part of the channel where the velocity distribution approaches the fully developed Hartmann profile, electrical dissipation is not properly accounted for, and in addition, viscous dissipation also becomes important at small Hartmann numbers.

Mention should be made of the relevance of laminar analyses to higher Reynolds numbers than are usually associated with channel flows without applied fields. Small disturbance, stability calculations reveal a strong stabilizing influence of a transverse magnetic field (Lock [20]). This is primarily because the fully developed Hartmann velocity profiles become steeper near the wall as the Hartmann number increases. Higher critical Reynolds numbers are predicted, and experimental measurements of friction factors by Murgatroyd [21] with mercury indicated laminar flow for Reynolds numbers $\bar{u}2a/\nu$ as high as approximately 50000 at a Hartmann number of approximately a hundred. More specifically, Murgatroyd suggests the transition Reynolds number $(\bar{u}2a/\nu)_{\text{Trans.}} \cong 450\,(Ha)$, a relation apparently not applicable to small Hartmann numbers.

A discussion of conditions that could occur in practice, i.e. the flow of real conducting fluids through channels that can be constructed and for actual fields that can be applied, is outside the scope of this paper. However, the information presented provides a basis for appraising the effect of fields on heat transfer in channel flows and should form a starting point for further analyses of other effects likely to occur in practice. For example, a more generalized Ohm's law for the electrical current j should be considered for plasma flows if Hall effects, ion slip effects, and pressure diffusion are important. To a first approximation from a heat-transfer standpoint, these effects would alter the electrical dissipation (j^2/σ), so that the Joule heating parameter S then is to be evaluated from the more general relation

$$S = \left(\frac{j^2}{\sigma}\right)\frac{EkPr}{(\bar{u}^2\mu/a^2)}.$$

REFERENCES

1. J. L. SHOHET, J. F. OSTERLE and F. Y. YOUNG, Velocity and temperature profiles for laminar magnetohydrodynamic flow in the entrance region of a plane channel, *Physics Fluids* **5**(5), 545–549 (1962).
2. L. E. ERICKSON, C. S. WANG, C. L. HWANG and L. T. FAN, Heat transfer to magnetohydrodynamic flow in a duct, *Z. Angew. Math. Phys.* **15**, 408–418 (1964).
3. I. MICHIYOSHI and R. MATSUMOTO, Heat transfer by Hartmann's flow in thermal entrance region, *Int. J. Heat Mass Transfer* **7**, 101–112 (1964).
4. C. W. TAN and K. SUH, Forced convection heat transfer in fully developed laminar flow of a hydromagnetic fluid, Report RE-201, Research Department, Grumman Aircraft Engineering Corp. (1965).

5. A. M. DHANAK, Heat transfer in magnetohydrodynamic flow in an entrance section, *J. Heat Transfer* **87**(2), 231–236 (1965).
6. S. D. NIGAM and S. N. SINGH, Heat transfer by laminar flow between parallel plates under the action of transverse magnetic field, *Q. Jl Mech. Appl. Math.* **13**, Part 1, 85–97 (1960).
7. G. W. SUTTON and A. SHERMAN, *Enginnering Magnetohydrodynamics*. McGraw-Hill, New York (1965).
8. P. J. SCHNEIDER, Effect of axial fluid conduction on heat transfer in the entrance regions of parallel plates and tubes, *Proc. Heat Transf. Fluid Mech. Inst.*, 41–57 (1956).
9. R. S. DE VOTO, Argon plasma transport properties, SUDAER No. 217, Department of Aeronautics and Astronautics, Standford University (1965).
10. E. R. G. ECKERT and R. M. DRAKE, *Heat and Mass Transfer*, 2nd edn., p. 299. McGraw-Hill, New York (1959).
11. R. H. NORRIS and D. D. STREID, Laminar-flow heat-transfer coefficients for ducts, *Trans. Am. Soc. Mech. Engrs* **62**(6), 525–533 (1940).
12. W. H. GIEDT, *Principles of Engineering Heat Transfer*, p. 155. Van Nostrand, Princeton, N.J. 1957.
13. R. ROIDT and R. D. CESS, An approximate analysis of laminar magnetohydrodynamic flow in the entrance region of a flat duct, *J. Appl. Mech.* **29**, 171–176 (1962).
14. C. L. HWANG and L. T. FAN, A finite difference analysis of laminar magnetohydrodynamic flow in the entrance region of a flat rectangular duct, *Appl. Scient. Res.* **B10**, 329–343 (1963).
15. W. T. SNYDER, Magnetohydrodynamic flow in the entrance region of a parallel-plate channel, *AIAA Jl* **3**, 1833–1838 (1965).
16. R. MANOHAR, An exact analysis of laminar magnetohydrodynamic flow in the entrance region of a flat duct, *Z. Angew. Math. Mech.* **46**, 111–117 (1966).
17. J. A. SHERCLIFF, Entry of conducting and nonconducting fluids in pipes, *Proc. Camb. Phil. Soc.* **52**, 573–583 (1956).
18. A. BRANDT and J. GILLIS, Magnetohydrodynamic flow in the inlet region of a straight channel, *Physics Fluids* **9**(4), 690–699, (1966).
19. M. F. ROMIG, The influence of electric and magnetic fields on heat transfer to electrically conducting fluids, *Adv. Heat Transf.* **1**, 309 (1964).
20. R. C. LOCK, The stability of the flow of an electrically conducting fluid between parallel planes under a transverse magnetic field, *Proc. R. Soc.* **A233**, 105–125 (1955).
21. W. MURGATROYD, Experiments on magnetohydrodynamic channel flow, *Phil. Mag.* **44**, 1348–1354 (1953).

Résumé—On présente les flux de chaleur pariétaux, les températures globales du fluide et les nombres de Nusselt calculés dans la région d'entrée thermique pour un écoulement laminaire uniforme et permanent d'un fluide à propriétés constantes et conducteur de l'électricité dans une conduite à plaques parallèles et à section droite constante avec des parois isothermes et non conductrices de l'électricité. On impose des champs magnétiques et électriques uniformes perpendiculairement entre eux et à l'écoulement. Les prévisions théoriques, tenant compte de la conduction longitudinale de la chaleur, dépendent de l'endroit le long de la conduite, du produit des nombres de Reynolds et de Prandtl (*Re Pr*) et du paramètre de chauffage par effet Joule *S*. L'importance du chauffage par effet Joule est montrée graphiquement. Les longueurs d'entrée thermique, proportionnelles à *Re Pr*, diminuent avec le chauffage par effet Joule et sont de l'ordre de la hauteur de la conduite pour de faibles valeurs de *Re Pr*. Les prévisions existantes des longueurs d'entrée pour la vitesse sont ajoutées dans un but de comparaison. On discute aussi de la région où le régime est entièrement établi.

Zusammenfassung—Berechnete Wärmeströme, Hauptstromtemperaturen und Nusselt-Zahlen werden angegeben für den thermischen Einlaufbereich bei stationärer, laminarer Strömung mit konstanten Stoffwerten in einem parallelwandigen Kanal gleichbleibenden Querschnitts mit isothermen, elektrisch nichtleitenden Wänden. Einheitliche magnetische und elektrische Felder werden senkrecht zueinander und zur Strömung aufgebracht. Die Berechnungen berücksichtigen Längswärmeleitung und hängen vom Ort des Kanals, vom Produkt von Reynolds- und Prandtl-Zahl (*Re Pr*) und vom Joule'schen Erwärmungsparameter *S* ab. Die Bedeutung der Joule'schen Erwärmung wird graphisch dargestellt. Die dem Produkt *Re Pr* proportionalen Einlauflängen nehmen mit der Joule'schen Erwärmung ab und liegen für kleine *Re Pr* in der Grössepordnung der Kanalhöhe. Zugleich sind bestehende Berechnungen für die hydrodynamische Einlauflänge angegeben. Der Bereich vollausgebildeter Strömung wird ebenfalls diskutiert.

Аннотация—Приводятся теоретические расчеты тепловых потоков на стенке, температур жидкости и чисел Нуссельта в термическом входном участке при стационарном однородном ламинарном течении электропроводящей жидкости с постоянными свойствами в плоско-параллельном канале постоянного поперечного сечения с изотермическими, электрически непроводящими стенками. Однородные магнитные и электрические поля расположены перпендикулярно друг к другу и к потоку. При анализе учитывается аксиальная теплопроводность, локальные значения осевой координаты, произведение чисел Рейнольдса и Прандтля (***Re Pr***) и параметр джоулева тепла ***S***.

На графике представлено влияние джоулева тепла. Термические входные участки, пропорциональные ***Re Pr***, сокращаются с уменьшением джоулева тепла при малых значениях проиведения ***Re Pr*** и по порядку величины равны высоте канала. Для сравнения приводятся существующие теоретические расчеты динамических входных участков. Также рассмотрена область полностью развитого течения.